Progress In Electromagnetics Research, PIER 101, 125–138, 2010

AN HYBRID MODEL FOR THE EVALUATION OF THE FULL-WAVE FAR-FIELD RADIATED EMISSION FROM PCB TRACES

A. G. Chiariello and G. Miano

DIEL
Universitá di Napoli Federico II
Via Claudio 21, 80125 Napoli, Italy

A. Maffucci

DAEIMI
Universitá di Cassino
Via G. Di Biasio 43, 03043 Cassino (FR), Italy

Abstract—The paper deals with the evaluation of the far-field radiated emissions from high-speed interconnects when the frequencies are such that the distribution of the currents along the traces is no longer of TEM-type. Instead of a computationally expensive numerical full-wave model, here a generalized transmission line model is used to obtain the current distributions. This full-wave transmission line model is derived from an integral formulation and is here extended to include in efficient way the layered media Green's Functions. The proposed tool is successfully benchmarked to references given in literature and case-studies of practical interest are carried out, referring to a coupled microstrip, driven either by differential and common mode currents. This analysis highlights the existence of a *transition* range where the error made by evaluating the emission using the classical transmission line current distribution is still negligible. Here a rule of thumb is derived which provides a simple criterion to estimate this extension of the range of validity of the classical transmission line.

1. INTRODUCTION

The study of the unwanted radiated emissions from PCB interconnects is a classical topic which has been deeply investigated in the past. Usually such interconnects have been described within the frame

Corresponding author: A. G. Chiariello (a.chiariello@unina.it).

of the circuit and/or the transmission line model. Due to the increasing signal frequencies, microstrip interconnects may exhibit non-negligible unwanted radiation which must be properly considered in the design and verification of high speed circuits (e.g., [1, 2]). For electrically short interconnects many semi-analytical models and simple formulas are available for the upper bounds of differential and common mode radiated emissions (e.g., [1, 3]). In nowadays high-speed PCBs operating in the GHz range some of the above models are inadequate and some of the classical results of the EMC analysis have to be revised. High-order effects have to be taken into account, related to finite size, discontinuities, parasitic modes and dielectric behavior. These effects are, in principle, catched only through a full-wave analysis. This kind of analysis could be performed through a full numerical model derived from any of the available numerical methods, like Finite Elements [4], Method of Moments [5] or Partial Element Equivalent Circuit [6]. For these applications integral approaches to Maxwells equations are widely used, because of their advantages over differential formulations: limited discretization region, naturally imposed regularity conditions and easy field-to-circuit coupling, *e.g.*, [7, 8]. The key point for an accurate evaluation of the fields is the use of the proper Green's function of the structure. Under reasonable approximations, for layered media it is possible to give closed form expressions to the Green's functions in spectral domain (*e.g.*, [9]), but their evaluation in the frequency domain has a high computational cost (*e.g.*, [10]). As a consequence, although a highly efficient implementation of these models may be obtained, the solution of the full-wave electromagnetic problem is computationally expensive and provides a low qualitative insight in the solution, since all the above effects are combined. Therefore, many authors have proposed hybrid approaches able to couple the accuracy of the full-wave models to the simplicity of the Transmission Line (TL) one [11–13]. An example of this approach is given in [13], where the radiated far field emitted by a differentially-driven microstrip is computed assuming that the current distribution along the traces is the TL model solution, i.e., assuming the propagation along the line to be of TEM type.

Following this stream, in this paper the Authors extend a recently proposed full-wave transmission line model in order to evaluate the far-field radiated emissions from PCBs when the frequencies are such that the propagation along the traces is no longer of TEM type. The starting point is the Enhanced Transmission Line (ETL) model [14–17], which provides the full wave current distribution in the frequency ranges of interest. This model has been presented in [14] and [16] for coupled microstrip with homogeneous dielectrics. A first attempt to

extend the model to inhomogeneous dieletrics is given in [17].

Section 2 is devoted to the integral formulation used for the far-field emission evaluation. A semi-analytical evaluation of the Green's functions is proposed, in order to obtain an accurate and efficient inclusion of the layered media. The approximated Green's Functions are then included in the ETL model for coupled microstrips, as shown in Section 3. The ETL model is then used to evaluate the full-wave current distribution along the traces. In Section 4, first a benchmark test is reported, then a case study is carried out, referring to a symmetric coupled microstrip. One of the results of this analysis is a practical criterion to establish an upper frequency bound to which the TL currents may still be used with negligible errors.

2. RADIATION FIELDS FROM PCB TRACES

Let us consider the microstrip of Fig. 1, of total length l, made by two signal conductors above a dielectric layer and a PEC ground plane. Let us assume the signal and ground trace to be ideal conductors and the slab to be made by ideal dielectric with dielectric constant ε, magnetic permeability μ and thickness h. Let $\mathbf{J}_s$ and σ_s indicate the superficial current and charge densities. In the frequency domain the magnetic vector potential $\mathbf{A}$ and the electric scalar potential φ may be computed at any position as follows:

$$\mathbf{A}(\mathbf{r}) = \mu_0 \iint_S G_A(\mathbf{r}, \mathbf{r}') \cdot \mathbf{J}_s(\mathbf{r}')\, dS, \tag{1}$$

$$\varphi(\mathbf{r}) = \frac{1}{\varepsilon_0} \iint_S G_\varphi(\mathbf{r}, \mathbf{r}')\, \sigma_s(\mathbf{r}')\, dS, \tag{2}$$

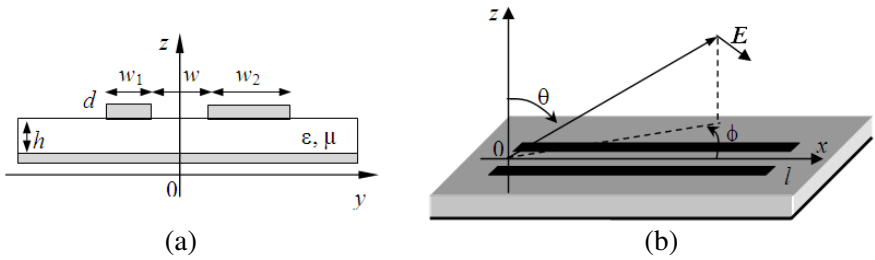

Figure 1. A coupled microstrip interconnect: (a) Cross-section; (b) references for the evaluation of the radiated electric field.

where G_A and G_φ are the *Green's functions* defined for the domain of interest, ε_0 and μ_0 are the vacuum space dielectric constant and magnetic permeability, S represents the union of all the surfaces S_k. The electric field is then given by

$$\mathbf{E} = -i\omega\mathbf{A} - \nabla\varphi, \tag{3}$$

in the following the *Lorenz gauge* is assumed. The evaluation of the Green function's is performed following the stream of what done in [16]. The G_A is in general dyadic, but if the conductors thickness is negligible and the current density may be assumed to be mainly directed along the longitudinal axis (x-axis), it reduces to the xx component G_A^{xx} only. A way to reduce the computational cost of the Green's functions is their decomposition in two parts:

- the *quasi-static* terms $G_{A,qs}$ and $G_{\varphi,qs}$
- the *dynamic* terms $G_{A,dyn}$ and $G_{\varphi,dyn}$

The first terms dominate the local range interactions, whereas the second ones dominate the far field zone. Similar decompositions are used in [21]. In this paper, we consider microstrip dimensions of the order of mm and frequencies up to 10 GHz. For these frequency and size ranges, according to the criterion given in [18], in evaluating the current distributions along the microstrip line we may approximate the complete Green's Functions with their quasi-static terms. This approximation reduces dramatically the computational cost, since the quasi-static terms may be evaluated analytically. The numerical computation of the dynamic parts, instead, would require a complex fitting procedure leading to at least around 10 cylindrical waves (Hankel functions), e.g., [18, 19].

Therefore, in the following we adopt the analitical approximations for the Green's Functions:

$$G_A(\rho; z, z') \approx G_{A,qs} = \frac{1}{4\pi}\frac{e^{-ik_0 r}}{r} - \frac{1}{4\pi}\frac{e^{-ik_0 r_1}}{r_1}, \tag{4}$$

$$G_\varphi(\rho; z, z') \approx G_{\varphi,qs} = \frac{1+K}{4\pi}\frac{e^{-ik_0 r}}{r} + \frac{K^2-1}{4\pi}\sum_{n=1}^{\infty} K^{n-1}\frac{e^{-ik_0 r_n}}{r_n}, \tag{5}$$

where ρ is the distance in the plane xy, z and z' are, respectively, the horizontal positions of the observe and the source, $k_0 = \omega\sqrt{\varepsilon_0\mu_0}$ is the vacuum space wavenumber and

$$r = \sqrt{\rho^2 + (z-z')^2}, \quad r_n = \sqrt{\rho^2 + d_n^2} \tag{6}$$

$$d_n = z + z' + 2nh, \qquad K = \frac{1-\varepsilon_r}{1+\varepsilon_r}. \tag{7}$$

In the far field zone, instead of computing the complete Green's functions, the parallel ray far field approximation is used because the trace widths are small with respect to the wavelength, i.e., $k_0 w_i \ll 1$, $i = 1, 2$. In this condition, according to [13], the far electrical field radiated from the n-th microstrip trace can be computed as follows:

$$E(r_n) = \frac{i\omega\mu_0}{4\pi}\frac{e^{-ik_0 r_n}}{r_n} \left[F_{xn}\int_0^l I_n(x)e^{ik_x x}dx + F_{zn}\int_0^h \left(I_n(0) - I_n(l)e^{ik_x l}\right)\cos(k_0\upsilon_n z)e^{ik_z z}dz\right], \quad (8)$$

where a local coordinate system $(r_n, \hat{\theta}_n, \phi_n)$ is defined, centered at one end of each trace, I_n is the current on the n-th microstrip

$$F_{xn} = (R_y - 1)\cos\theta_n \cos\phi_n\, \hat{\theta} + (R_h - 1)\sin\phi_n\, \hat{\phi}, \quad (9)$$

$$R_y = \frac{1 - i\frac{\upsilon_n}{\varepsilon_r \cos\theta_n}\tan(k_0\upsilon_n h)}{1 + i\frac{\upsilon_n}{\cos\theta_n}\tan(k_0\upsilon_n h)}, \quad (10)$$

$$R_h = \frac{1 + i\frac{\upsilon_n}{\cos\theta_n}\cot(k_0\upsilon_n h)}{1 - i\frac{\upsilon_n}{\cos\theta_n}\cot(k_0\upsilon_n h)}, \quad (11)$$

$$F_{zn} = \frac{(R_y + 1)\sin\theta_n}{\varepsilon_r \cos(k_0\upsilon_n h)}\,\hat{\theta}, \quad (12)$$

$$\upsilon_n = \sqrt{\varepsilon_r - \sin^2\theta_n}. \quad (13)$$

If the dielectric is *electrically thin* compared to the wavelength (i.e., if $h \ll \lambda$), Equation (8) becomes

$$E(r_n) = \frac{i\omega\mu_0}{4\pi}\frac{e^{-ik_0 r_n}}{r_n}\left[F_{xn}\int_0^l I_n(x)e^{ik_x x}dx + F_{zn}\left(I_n(0) - I_n(l)e^{ik_x l}\right)h\right], \quad (14)$$

The total electrical field is $E = \sum_{n=1}^{2} E(r_n)$. If the propagation along the microstrip is of TEM type the current distribution along the trace is provided by the TL solution and Equation (14) may be analytically evaluated [13].

3. CURRENT DISTRIBUTIONS

The full-wave current distributions along the traces of the microstrip in Fig. 1 may be obtained numerically with different approaches (MoM, FEM, BEM techniques), which usually do not provide qualitative

insight in the solution. An elegant alternative is given by the use of generalized TL models, which extend to full-wave ranges the validity of the classical TL solutions. An enhanced transmission line (ETL) model able to describes the conditions analyzed in this paper has been proposed by the Authors in [14–17]. Let us denote with $\mathbf{I}(x)$, $\mathbf{V}(x)$, $\mathbf{Q}(x)$ and $\mathbf{\Phi}(x)$ the vectors of the current, voltage, electrical charge and magnetic flux distributions, per unit length (p.u.l.), along the line. The ETL model is given by the following equations:

$$\frac{d\mathbf{I}\,(x)}{dx} + i\omega\mathbf{Q}\,(x) = 0, \quad -\frac{d\mathbf{V}\,(x)}{dx} = i\omega\mathbf{\Phi}\,(x)\,, \tag{15}$$

$$\mathbf{\Phi}(x) = \mu_0 \int_0^l H_I(x-x')\mathbf{I}(x)dx', \tag{16}$$

$$\mathbf{V}(x) = \frac{1}{\varepsilon_0}\int_0^l H_Q(x-x')\mathbf{Q}(x)dx'. \tag{17}$$

In the Standard Transmission Line (STL) model, relations (16) and (17) are replaced by the usual local relations

$$\mathbf{\Phi}(x) = L\mathbf{I}(x), \quad \mathbf{V}(x) = C^{-1}\mathbf{Q}(x), \tag{18}$$

being L and C the p.u.l. inductance and capacitance matrices, respectively. Therefore the ETL model differs from the STL in the spatial dispersion introduced by the convolutions in Equations (16), (17), whose kernels are given by the matrices:

$$H_I^{ip}(\zeta) \;=\; \frac{1}{c_i}\oint_{l_i} ds_i \oint_{l_p} G_A\left(s_i, s_p'; \zeta\right) F_i\left(s_p'\right) ds_p', \tag{19}$$

$$H_Q^{ip}(\zeta) \;=\; \frac{1}{c_i}\oint_{l_i} ds_i \oint_{l_p} G_\varphi\left(s_i, s_p'; \zeta\right) F_i\left(s_p'\right) ds_p', \tag{20}$$

with $p, i = 1, 2$. Here l_m, c_m and s_m (with $m = p, i$) are respectively the cross-section contour of the generic conductor, its length and a curvilinear abscissa along it.

This approach is possible when the characteristic transverse dimensions of the conductors are *electrically short*, (i.e., when $(t \ll \lambda)$) and the characteristic dimensions of the terminal devices are small compared to the interconnect length. Assuming the dielectric thickness h (see Fig. 1) as the characteristic dimension in the cross section, the above condition sets the highfrequency validity limit for the ETL model:

$$kh \approx 5, \tag{21}$$

being k the wavenumber, which could be expressed in terms of the propagation velocity c:

$$k = \frac{\omega}{c}, \tag{22}$$

When the frequency goes to zero and the interconnect length goes to infinity, this model reduces to the STL one. The upper frequency bound for the STL is given by [17]:

$$kh \approx 0.1 \tag{23}$$

For lower frequencies, the solutions obtained from STL and ETL models agree. For the evaluation of the emissions it is useful to recast the problem in terms of differential and common mode components, usually denoted as mixed-mode variables. To this purpose let us define the differential model variables as follows:

$$I_d(x) \equiv \frac{I_1(x) - I_2(x)}{2}, \qquad V_d(z) \equiv V_1(x) - V_2(x), \tag{24}$$

$$Q_d(x) \equiv \frac{Q_1(x) - Q_2(x)}{2}, \quad \Phi_d(x) \equiv A_1(x) - A_2(x), \tag{25}$$

and the common mode variables as:

$$I_C(x) \equiv I_1(x) + I_2(x), \qquad V_C(x) \equiv \frac{V_1(x) + V_2(x)}{2}, \tag{26}$$

$$Q_c(x) \equiv Q_1(x) + Q_2(x), \quad \Phi_c(x) \equiv \frac{A_1(x) + A_2(x)}{2}. \tag{27}$$

The mixed-mode STL model is simply given by:

$$\frac{d\mathbf{I}_M(x)}{dx} = -i\omega \mathrm{C_M}\mathbf{V}_M, \quad \frac{d\mathbf{V}_M(x)}{dx} = -i\omega \mathrm{L_M}\mathbf{I}_M(x), \tag{28}$$

where the common and differential mode voltage $\mathbf{V}_M(x)$ and current vectors $\mathbf{I}_M(x)$ and are defined according to Equations (24)–(27) and the p.u.l. mixed mode matrices, are given by

$$\mathrm{C_M} = \mathrm{ACB}^{-1}, \quad \mathrm{L_M} = \mathrm{BLA}^{-1}, \tag{29}$$

being

$$\mathrm{A} = \begin{bmatrix} 1/2 & -1/2 \\ 1 & 1 \end{bmatrix}, \quad \mathrm{B} = \begin{bmatrix} 1 & -1 \\ 1/2 & 1/2 \end{bmatrix}. \tag{30}$$

In the general case, the differential and common modes propagate with different velocities and characteristic impedances. The velocities c_{CM} and c_{DM} may be computed as $1/\sqrt{\lambda_k}$, $k = 1, 2$, where λ_k are the eigenvalues of the matrix $L_M C_M$. This approach is rigorous for symmetric interconnects, like in our case-study, since the common and differential modes are decoupled. For asymmetric interconnects

this procedure gives approximated values of the velocities. In the following we use the velocity $c = \min\{c_{CM}, c_{DM}\}$ for evaluating the frequency ranges. From condition (23), the frequency f_0 above which the propagation could no longer be described by the STL model is:

$$f_0 \approx 0.0159 \frac{c}{h}. \tag{31}$$

Note that the ETL model itself may be easily recast in terms of these mixed-mode variables, as shown in [16].

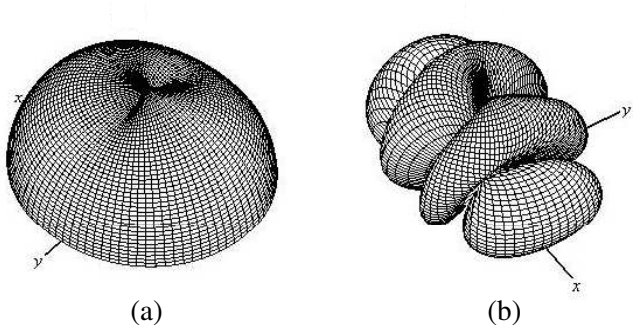

Figure 2. Benchmark test: Radiation diagrams for (a) 0.08 GHz, $l\backslash\lambda = 0.05$ and (b) 4.94 GHz, $l/\lambda = 3$.

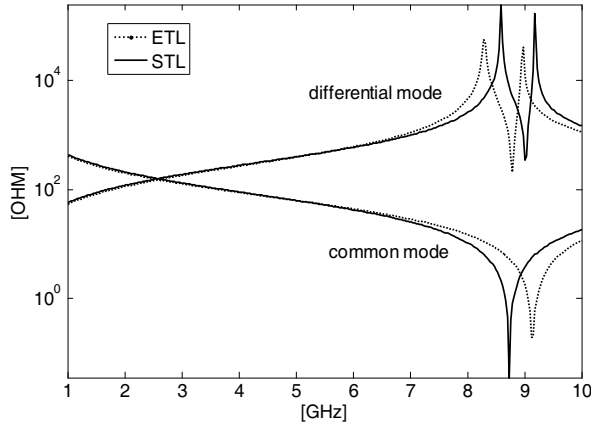

Figure 3. Case-study: STL and ETL solutions for the differential and common mode input impedances.

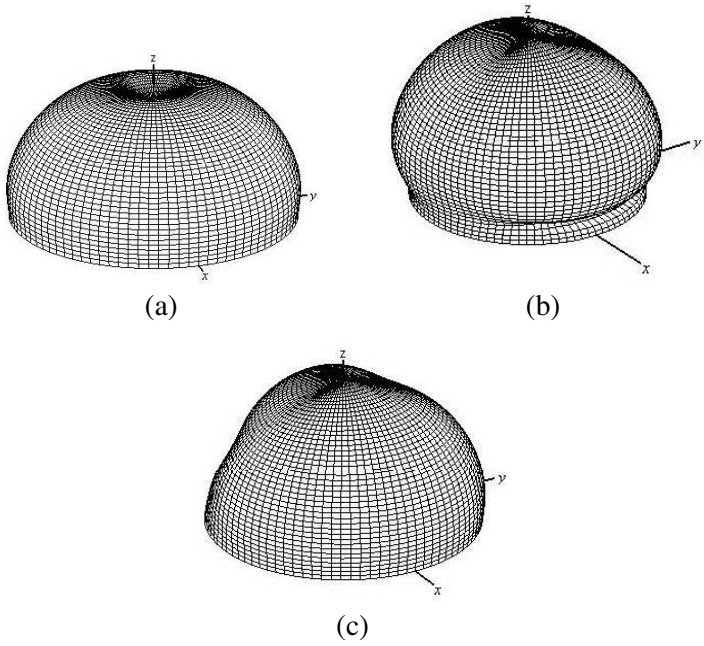

Figure 4. Case-study, radiation diagrams: (a) 5 GHz, STL and ETL; (b) 9 GHz, ETL; (c) 9 GHz, STL.

4. RESULTS

The accuracy and consistency of the distribution of currents provided by the ETL model has been deeply analyzed in [17]. Therefore in the following the solution obtained by using the ETL current distribution will be assumed as the full-wave solution. Here a benchmark test is carried out with the only purpose to validate the procedure (8)–(14) leading to the far-field computation. The test case is taken from [13] and refers to a single-trace microstrip with $w = 0.51$ cm, $h = 0.775$ mm a total length of 10.16 cm, $\varepsilon_r = 4.6$. Let us assume the boundary conditions: $I(x = 0) = 1$ [a.u.] and $I(x = l) = 0$. In Fig. 2, we show the radiation diagram computed at 0.08 GHz and 4.94 GHz: these conditions correspond to those analyzed in ([13]), reported as $l\backslash\lambda = 0.05$, $l\backslash\lambda = 3$ and $\rho_L = 1$. A satisfactorily agreement between Fig. 2 and the results shown in ([13]) is obtained. Similar results may be obtained for the other cases analyzed in this reference.

Let us now investigate the case-study of a symmetric microstrip with typical dimensions [20]: $w = w_1 = w_2 = 0.1$ mm, $h = 1$ mm, a

total length of 10 mm, ideal conductors and $\varepsilon_r = 4.4$. Fig. 3 shows the input impedance of the coupled line, computed for a differential mode and for a common mode feeding at $x = 0$ (the terminations at $x = l$ are left open). Condition (31) provides an upper frequency limit for the STL solution which is 2.7 GHz. However, Fig. 3 suggests that the STL solution may be used for higher frequencies, since it deviates from the full-wave one only when approaching the first resonances. Let us refer to the emitted fields computed at a distance of 3 m (far-field region). Fig. 4 shows the radiation diagrams evaluated at 5 and 9 GHz, assuming a differential mode feeding: $I_{DM}(x = 0) = 1$ mA (the

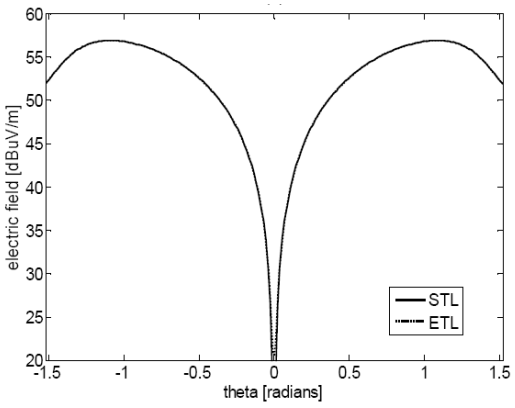

Figure 5. Radiated field in the plane x-z at 5 GHz (differential mode).

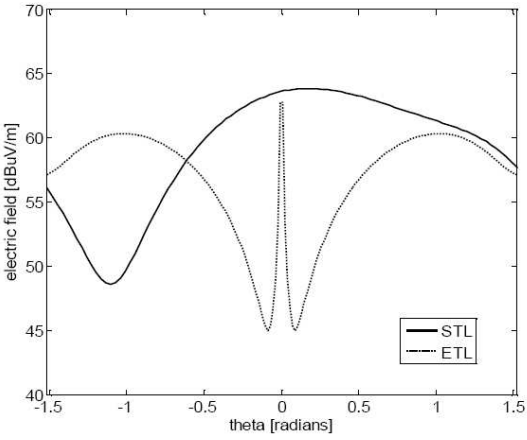

Figure 6. Radiated field in the plane x-z at 9 GHz (differential mode).

terminations at $x = l$ are left open). At 5 GHz the approximated solution obtained by using the STL current distribution along the traces agree with the full-wave one (Fig. 4(a)), whereas some differences may be observed at 9 GHz (Figs. 4(b) and 4(c)). In order to appreciate better these differences, let us cut the radiation diagrams in the plane x-z, as in Figs. 5, 6. Now the difference at 9 GHz between the two solution is more evident.

The same behavior may be observed for the common-mode ($I_{CM}(x = 0) = 1$ mA), see Figs. 7, 8.

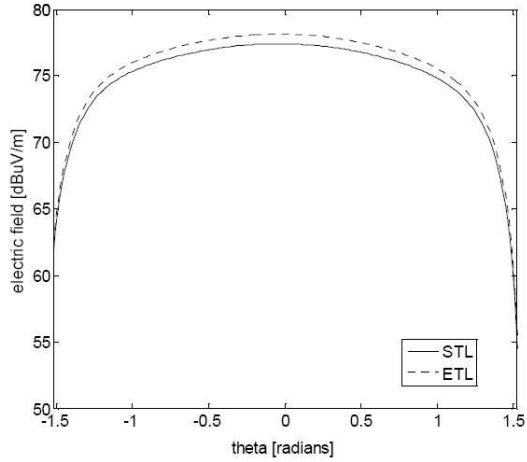

Figure 7. Radiated field in the plane x-z at 5 GHz (common mode).

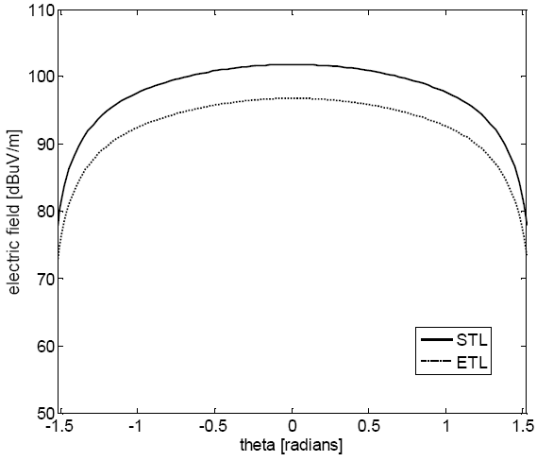

Figure 8. Radiated field in the plane x-z at 9 GHz (common mode).

The above results confirm that the STL solution may be used also in non-TEM ranges if the frequency is enough far from the resonances. The resonance frequencies in a coupled microstrip as the one in Fig. 1 are in general different for the two modes, since their velocities are different. Once again, assuming $c = \min\{c_{CM}, c_{DM}\}$ the first resonance for a line of length l occurs at

$$f_r = \frac{c}{2l}. \tag{32}$$

Therefore we propose the following simple rule of thumb: compute the frequencies f_0 and f_r: if $f_0 < f_r$ we can keep on using the STL solution for frequencies up to f_r. For the analyzed case-study we have $f_0 = 2.7\,\text{GHz}$ and $f_r = 8.6\,\text{GHz}$. Note that f_r is strongly influenced by the line length. If we assume $l = 30\,\text{mm}$ we get $f_r = 2.9\,\text{GHz}$, hence limiting the range where we can still use the STL solution. Fig. 9 shows the radiated field in the x-y plane solution at 3 GHz for the differential mode: it is evident that for this frequency we can no longer use the STL solution.

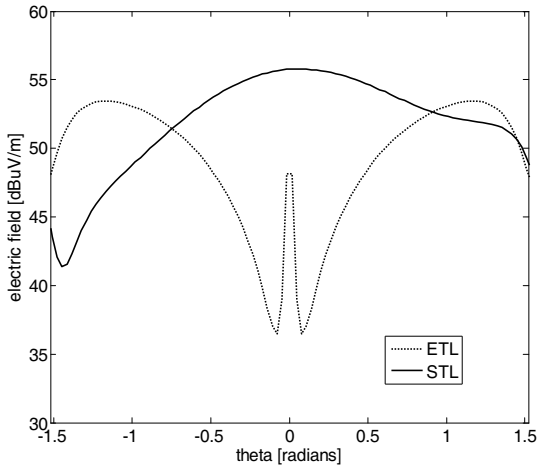

Figure 9. Radiated field in the plane x-z at 3 GHz (differential mode, length $l = 30\,\text{mm}$).

5. CONCLUSIONS

In this paper, the far field emission from high-speed PCB interconnects is evaluated by means of an hybrid model, which conjugates the simplicity of the transmission line model to the accuracy of a full-wave solution. Indeed the current distributions along the traces are obtained

from a generalized transmission line model, which is here enhanced by means of an efficient inclusion of the layered Green's Functions. Using these currents, the far field emission is computed by using the parallel ray far field approximation. Among the other results, a simple criterion is established, to check whether the classical transmission line solution may be still adopted although in non-TEM frequency ranges.

REFERENCES

1. Paul, C. R., *Introduction to Electromagnetic Compatibility*, Wiley, New York, 1992.
2. Gravelle, L. B. and P. F. Wilson, "EMI/EMC in printed circuit boards — A literature review," *IEEE TEMC*, Vol. 34, 109–116, 1992.
3. Paul, C. R., "A comparison of the contributions of common-mode currents and differential-mode currents in radiated emissions," *IEEE TEMC*, Vol. 31, No. 2, 189–193, 1989.
4. Matias, R. M. and A. Raizer, "Calculation of electric field created by transmission lines, by 3D-FE method using complex electric scalar potential," *ACES, Journal*, Vol. 12, No.1, 56–60, 1997.
5. Naishadham, K., J. B. Berry, and H. A. N. Hejase, "Full-wave analysis of radiated emission from arbitrarily shaped printed circuit traces," *IEEE TEMC*, Vol. 35, No. 3, 366–377, 1993.
6. Pinello, W. P., A. C. Cangellaris, and A. Ruehli, "Prediction of differential- and common-mode noise in high-speed interconnects with the partial element equivalent circuit technique," *IEEE Intern. Sympos. on EMC*, Vol. 2, 940–945, Aug. 1998.
7. Mosig, J., "Arbitrarily shaped microstrip structures and their analysis with a mixed potential integral equation," *IEEE Trans. Microwave Theory Tech.*, Vol. 36, 314–323, Feb. 1988.
8. Zhao, J. S. and W. C. Chew, "Integral equation solution of Maxwells equations from zero frequency to microwave frequencies," *IEEE TAP*, Vol. 48, No. 10, 1635–1645, Oct. 2000.
9. Chew, W. C., *Waves and Fields in Inhomogeneous Media*, IEEE Press, 1996.
10. Abdelmageed, A. K. and M. S. Ibrahim, "On enhancing the accuracy of evaluating Green's functions for multilayered media in the near-field region," *Progress In Electromagnetics Research M*, Vol. 2, 1–14, 2008.
11. Jerse, T. A. and C. Paul, "A hybrid method for efficient estimating common-mode radiation from transmission-line structures," *Proc.*

of EM International Symposium Record, 145–149, Atlanta, Aug. 1995.

12. Chen, I. F., C. M. Peng, and C. W. Hsue, "Circuit-concept approach to radiated emissions of printed circuit boards," *IEE Proc. Sci. Meas. Tech.*, Vol. 151, No. 3, 205–210, 2004.
13. Leone, M., "Closed-form expressions for the electromagnetic radiation of microstrip signal traces," *IEEE TEMC*, Vol. 49, 322–328, 2007.
14. Maffucci, A., G. Miano, and F. Villone, "Recent developments of transmission line models for interconnects," *PIRES Proceedings*, 97–100, Pisa, Italy, Mar. 28–31, 2004.
15. Maffucci, A., G. Miano, and F. Villone, "An enhanced transmission line model for conductors with arbitrary cross-sections," *IEEE TAdvP*, Vol. 28, 174–188, 2005.
16. Chiariello, A. G., A. Maffucci, G. Miano, F. Villone, and W. Zamboni, "A transmission-line model for full-wave analysis of mixed-mode propagation," *IEEE TAdvP*, Vol. 31, No. 2, 275–284, 2008.
17. Chiariello, A. G., A. Maffucci, G. Miano, and F. Villone, "Transmission line models for high-speed conventional interconnects and metallic carbon nanotube interconnects," *Electromagnetic Field Interaction with Transmission Lines*, F. Rachidie and S. Tkachenko (eds.), WIT Press, Southampton, UK, Feb. 2008.
18. Chow, Y. L., J. J. Yang, D. G. Fang, and G. E. Howard, "A closed-form spatial Green's function for the thick microstrip substrate," *IEEE T-MTT*, Vol. 39, 588–592, 1991.
19. Michalski, K. A. and J. R. Mosig, "Multilayered media Green's functions in integral equation formulations," *IEEE T-AP*, Vol. 45, No. 3, 508–519, 1997.
20. Sharma, R., T. Chakravarty, and A. B. Bhattacharyya, "Signal integrity issues in high-speed interconnects over a ground plane aperture," *Journal of Electromagnetic Waves and Applications*, Vol. 22, No. 16, 2231–2240, 2008.
21. Essid, C., M. B. B. Salah, K. Kochlef, A. Samet, and A. B. Kouki, "Spatial-spectral formulation of method of moment for rigorous analysis of microstrip structures," *Progress In Electromagnetics Research Letters*, Vol. 6, 17–26, 2009.